



Unveiling LDL dynamics post-stent intervention: a deep dive into transport and accumulation

ZHENMIN FAN¹, TONGYU ZHAN¹, XIA YE^{1*}, XIAOYAN DENG², XIAO LIU^{2*}, SHENGZHAO XIAO^{3*}

¹ School of Mechanical Engineering, Jiangsu University of Technology, Changzhou Jiangsu, China.

² Key Laboratory for Biomechanics and Mechanobiology of Ministry of Education,
School of Biological Science and Medical Engineering, Beihang University, Beijing, China.

³ Department of Orthodontics, Shanghai Ninth People's Hospital, Shanghai Jiao Tong University School of Medicine;
College of Stomatology, Shanghai Jiao Tong University; National Center for Stomatology;
National Clinical Research Center for Oral Diseases; Shanghai Key Laboratory of Stomatology;
Shanghai Research Institute of Stomatology. Shanghai, China.

The endovascular stent implantation is a significant and efficacious cardiovascular interventional treatment. However, the underlying mechanisms behind in-stent neoarteriosclerosis and restenosis following the intervention remain unclear. Our hypothesis posits that stent implantation may impact the transportation of low-density lipoproteins (LDL) within the host artery, thereby disrupting its concentration distribution and leading to adverse clinical events. To validate this hypothesis, we conducted a numerical investigation to examine the influence of stenting on LDL distribution, utilizing a lumen-wall model based on the coronary artery. The findings of the study suggest that the introduction of an implanted stent can disrupt blood flow and result in an abnormal accumulation of lipids on the inner surface of the arterial wall, particularly in the vicinity of the strut protrusion. Additionally, improper stent implantation, characterized by thick struts, reduced spacing between struts, and non-streamlined struts can exacerbate the local mechanical conditions of the host artery and contribute to a relatively high concentration of low-density lipoprotein (LDL) near the stent strut. In summary, the presence of a stent in the artery leads to an elevated LDL concentration both within the stented segment and downstream, potentially leading to adverse consequences.

Key words: low-density lipoproteins, hemodynamics, stents, restenosis, thrombosis

1. Introduction

Stenting intervention is a widely accessible and efficacious approach for the treatment of stenotic atherosclerosis, particularly in cases of coronary stenosis. Nonetheless, this intervention may give rise to clinical cardiac events in the course of post-stenting follow-up. The compromised advantages of this strategy serve as clinical evidence of the comparatively elevated risks associated with recurrent stenosis, neoarteriosclerosis and thrombosis [9], [10]. According to

clinical data, the restenosis rates of stent implantation ranged from 16 to 44% [35] and late stent thrombosis accounted for approximately 1%, but caused more than 90% of the disability or death [30].

The incidence of adverse events following stent implantation is intricately linked to the altered mechanical conditions within the host artery. The alterations induced by stenting result in significant damage to the arterial wall, particularly affecting the vascular endothelial cells, as a consequence of the compressive forces exerted by the stent struts. This process subsequently triggers vascular remodeling, inflammation and heal-

* Corresponding authors: Shengzhao Xiao, Department of Orthodontics, Shanghai Ninth People's Hospital, Shanghai Jiao Tong University School of Medicine; College of Stomatology, Shanghai Jiao Tong University; National Center for Stomatology; National Clinical Research Center for Oral Diseases; Shanghai Key Laboratory of Stomatology; Shanghai Research Institute of Stomatology, e-mail: shengzhaoxiao@shsmu.edu.cn; Xia Ye, School of Mechanical Engineering, Jiangsu University of Technology, Changzhou Jiangsu, China, e-mail: yx_laser0@163.com

Received: October 25th, 2024

Accepted for publication: January 15th, 2025

ing [15]. Furthermore, the presence of protruding stent struts can disrupt the flow within the lumen, leading to stagnation and separation of the fluid around these struts [17]–[29]. This unfavorable fluid behavior primarily contributes to vascular injury and the development of recurrent stenosis and thrombosis. The initial occurrence of in-stent restenosis can be attributed to damage to the vascular wall and loss of endothelial cells, particularly in the vicinity of the stented segment. This endothelial denudation and dysfunction serve as significant factors in the occurrence of injury events and subsequent adverse outcomes [24].

The destruction of endothelial cells and the glycocalyx layer has the potential to expedite the infiltration and buildup of detrimental macromolecules, including LDL, within the arterial wall [15], [33]. Experimental evidence has shown that the heightened water conductivity and permeability of endothelial cells result in swift macromolecule accumulation in the intima, following their destruction [36], [37]. Furthermore, the restoration of endothelial function subsequent to percutaneous coronary interventions is inadequate, as evidenced by compromised intercellular junctions, heightened permeability and increased hydraulic conductivity [24]. These studies have demonstrated that endothelial incompetence and/or dysfunction at the stented segment can significantly augment LDL transport, resulting in heightened deposition and accumulation of LDL within the arterial wall. The accumulation of lipids within the arterial wall has been established as a crucial factor in the initiation and progression of atherosclerosis. Consequently, the elevated presence of LDL in the intima may be associated with an increased burden of plaque, ultimately contributing to the accelerated development of in-stent neoatherosclerosis [11]. In contrast to atherosclerosis occurring in native arteries, the accelerated development of neoatherosclerosis in the stented segment is characterized by the presence of lipid-rich and atherosclerotic yellow neointima. This neointima serves as a crucial factor contributing to stenting failure. Postmortem investigations have consistently observed the frequent occurrence of lipid-laden intima in lesions that have undergone sirolimus-eluting or bare-metal stent placement, particularly in the later stages [22].

Additionally, the presence of external factors, such as significant impairment to vascular endothelial cells and the specific design of the stent, can exacerbate and expedite the development of neoatherosclerosis lesions. As previously stated, the size of the stent's struts, the spacing between them and the overall shape of the struts have been found to be correlated with the formation of vortices or the extent of disrupted blood flow

subsequent to the intervention [1]. Furthermore, research indicate that an optimized stent design can result in improved blood flow patterns, thereby enhancing the efficacy of the intervention while minimizing the occurrence of in-stent thrombosis and restenosis [2]–[28].

Since the in-stent atherogenesis after the intervention is similar to that in the native artery, accelerated neoatherosclerosis in the stented segment has been associated with the mass transport and distribution of atherogenic lipids [8]. Elevated hydraulic conductivity and water filtration rate across the arterial wall in the stented segment, and higher residence time of atherogenic lipids at a high level are proposed to account for accelerated atherogenesis after the intervention. Current work numerically simulated LDL mass transport in models after interventions and compared the impact of different damage degrees on host arterial wall on LDL distribution to verify our hypothesis. The change in LDL concentration due to different stenting scenarios was also discussed.

The occurrence of in-stent atherogenesis following the intervention bears resemblance to that observed in the native artery, and it has been linked to the transportation and dispersion of atherogenic lipids. The accelerated development of neoatherosclerosis in the stented segment is hypothesized to be influenced by increased hydraulic conductivity and water filtration rate across the arterial wall within this segment, as well as prolonged exposure of atherogenic lipids at elevated concentrations. The present study employed numerical simulations to investigate the transport of LDL mass in models following interventions, and to assess the influence of varying degrees of damage to the host arterial wall on LDL distribution, thereby validating our hypothesis. Additionally, the alteration in LDL concentration resulting from different stenting scenarios was also examined and discussed.

2. Methods

2.1. Geometry of computational model

In Figure 1, the computational models to investigate LDL concentration in stented coronary is displayed. The ideal artery was simplified as a cylinder (two dimension) with a length of 60 mm, and thickness of arterial wall and the outer diameter of artery were set to be 0.34 and 3.7 mm, which were in accor-

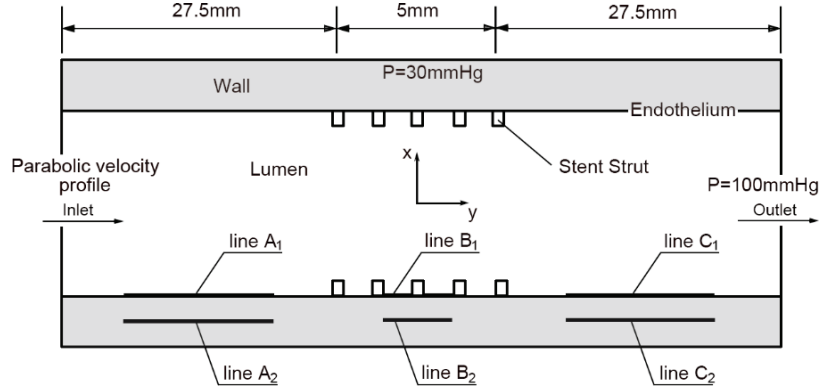


Fig. 1. Schematic illustration of computational model after the stent intervention.

Representative lines for the numerical data postprocessing. Line A, B and C lie at the upstream, middle and downstream of the stented segment. Here subscript 1 indicates on luminal surface wall artery wall, while 2 indicates in the arterial wall

dance with size of the human left coronary artery [7]. Implanted stent was emplaced in the middle of artery and was simplified as a ten independent rectangle struts ($0.162 \text{ mm} \times 0.081 \text{ mm}$, named N in Table 1) without connection, the distance between struts was 1 mm [16]. To study the effect of stent thickness, stent strut thicknesses were $162.0 \text{ }\mu\text{m}$ (N), $145.8 \text{ }\mu\text{m}$ (T1) and $121.5 \text{ }\mu\text{m}$ (T2). To study the impact of strut spacing, the distance between struts is $1000 \text{ }\mu\text{m}$ (N), $2000 \text{ }\mu\text{m}$ (S2) and $4000 \text{ }\mu\text{m}$ (S2). To study the influence of strut shape on the LDL distribution, streamlined stent strut shaped elliptical was constructed.

Table 1. Stent struts parameter [μm]

Strut name	Thickness	Spacing	Strut shape
N	162.0	1000	rectangles
T1	145.8	1000	rectangles
T2	121.5	1000	rectangles
S1	162.0	2000	rectangles
S2	162.0	4000	rectangles
S3	162.0	2000	elliptical

2.2. Numerical approaches

2.2.1. Fluid dynamics

Lumen

Numerical simulations for blood flow in arterial lumen was performed based on the two-dimensional (2D), incompressible Navier–Stokes equation and continuity equation [39].

$$\rho_l \left(\frac{\partial \mathbf{u}_l}{\partial t} + \mathbf{u}_l \cdot \nabla \mathbf{u}_l \right) = -\nabla p_l + \nabla \cdot \boldsymbol{\tau}, \quad (1)$$

$$\nabla \cdot \mathbf{u}_l = 0, \quad (2)$$

where ρ_l ($\rho_l = 1050 \text{ kg/m}^3$) and $\boldsymbol{\tau}$ stand respectively for the density and the stress tensor [21]. The two-dimensional velocity vector and pressure in the arterial lumen are represented by \mathbf{u}_l and p_l , respectively.

$$\boldsymbol{\tau} = 2\mu(\dot{\gamma})\mathbf{S}, \quad (3)$$

where $\dot{\gamma}$ and \mathbf{S} stand respectively the shear rate and for the rate of deformation tensor. The viscosity of blood flow was described by Carreau model [32].

$$\mu(\dot{\gamma}) = \mu_\infty + (\mu_0 - \mu_\infty) [1 + (\lambda \dot{\gamma})^2]^{\frac{n-1}{2}}, \quad (4)$$

where μ_∞ and μ_0 represent respectively the viscosity at infinite shear rate ($\mu_\infty = 0.00345 \text{ kg/(ms)}$) and at zero shear rate ($\mu_0 = 0.056 \text{ kg/(ms)}$), λ stands for the time constant ($\lambda = 3.31 \text{ s}$) and n stands for the power law index ($n = 0.36$).

Endothelium

The solution of Kedem–Katchalsky equation was applied for the simulation of the transmural fluid flow across the endothelium (J_v) [31].

$$J_v = L_p(\Delta p - \sigma \Delta \pi), \quad (5)$$

where L_p stands for the hydraulic conductivity of endothelium, J_v is the volume flux, σ is the endothelium osmotic reflection coefficient. Since the influence of osmotic pressure on fluid flow is negligible compared to the hydrostatic pressure difference across the endothelial layer. $\Delta \pi$ in this study stand for the oncotic pressure difference neglected in the present simulation, the pressure drop is Δp .

Arterial wall

Darcy's Law coupled with continuity equations was applied for the transmural fluid flow across the host arterial wall.

$$\frac{\mu_w}{K_w} u_w = -\nabla(p_w), \quad (6)$$

$$\nabla \cdot u_w = 0, \quad (7)$$

where p_w and u_w for pressure and velocity vector on the arterial wall, K_w represents the hydraulic permeability ($1.34 \times 10^{-18} \text{ m}^3$), and μ_w is viscosity of blood flow ($7.2 \times 10^{-4} \text{ kg/(ms)}$).

2.2.2. Solute dynamics

Lumen

LDL transport in blood was modeled by the convection–diffusion equations[19].

$$u_l \cdot \nabla c_l - D_l \Delta c_l = 0, \quad (8)$$

where c_l stands for LDL concentration in the arterial lumen, D_l is the LDL diffusion coefficient in blood flow ($5.898 \times 10^{-12} \text{ m}^2/\text{s}$) [20].

Endothelium

The Kedem–Katchalsky equation was be used to describe LDL flux across the endothelium(J_s) [19].

$$J_s = P_{\text{end}} \Delta c_l + (1 - \sigma_f) J_v c_m, \quad (9)$$

where Δc_l stands for LDL concentration difference after cross endothelium, P_{end} stands for the LDL permeability, σ_f represents LDL reflection coefficient, c_m stands for the mean concentration on both sides of the endothelium ($c_m = 0.997$).

Arterial wall

The transport of LDL in the host artery wall was given by the convection–diffusion–reaction equation [31].

$$\nabla \cdot (-D_w \nabla c_w + K_{\text{lag}} c_w u_w) = r_w c_w, \quad (10)$$

where D_w stands for the LDL effective diffusivity in arterial wall ($D_w = 1.42 \times 10^{-12} \text{ m}^2/\text{s}$), K_{lag} represents LDL lag coefficient ($K_{\text{lag}} = 0.1486$), and r_w is the LDL chemical reaction rate ($r_w = -6.05 \times 10^{-4} \text{ s}^{-1}$).

2.2.3. Boundary conditions

Blood flow

A parabolic velocity waveform with an average value of 0.24 m/s was applied at the computational

model inlet for the pulsating flow [13]. 100 mmHg was set at the computational model outlet, and a constant 30 mmH was applied the outer arterial wall, which are from the healthy intravascular pressure [36]. The endothelium boundary on one side of the lumen (the wall to lumen transmural velocity of fluid) was set to be J_v , and the other side of the wall was set to be $-J_v$ [37].

LDL

Concentration of LDL (c_0) was chosen to be $2.86 \times 10^2 \text{ mol/m}^3$ at the inlet of arterial lumen [37]. The endothelium boundary on one side of the lumen (the wall to lumen flux of LDL) was set to be J_s , the other side of the wall was set to be $-J_s$.

2.2.4. Computation procedures

The numerical simulations were finished in COMSOL Multiphysics by a validated finite element algorithm. The flow simulation was first carried out for velocity and pressure fields, which then served for the simulation of LDL transport. The triangular mesh was applied for the computational study, the elements size of the lumen was 0.2 mm, and the vessel wall was 0.08 mm, the elements near the stent were refined, and the boundary layer of the fluid domain was set to 15 layers. MUMPS solver was used in for all cases in this work. The density of the mesh is a critical factor influencing the accuracy of numerical calculations. Accordingly, this study developed five models with progressively increasing mesh densities, ranging from 50 000 to 500 000 cells. The results indicate that the relative error between two cases drops below 5% when the number of mesh cells exceeds 300 000, thereby confirming the grid independence. Consequently, the results obtained with this mesh density are used for subsequent analysis.

3. Results

3.1. Effect of the stenting

In Figure 2A, the axial distribution of LDL in the coronary artery is shown. Compared to the model without intervention, implanted stent would significantly increase the concentration of LDL near stent strut, especially for the stent strut downstream edge, where the strut would lead to flow disruption, causing flow stagnation and recirculation. LDL concentration near stent

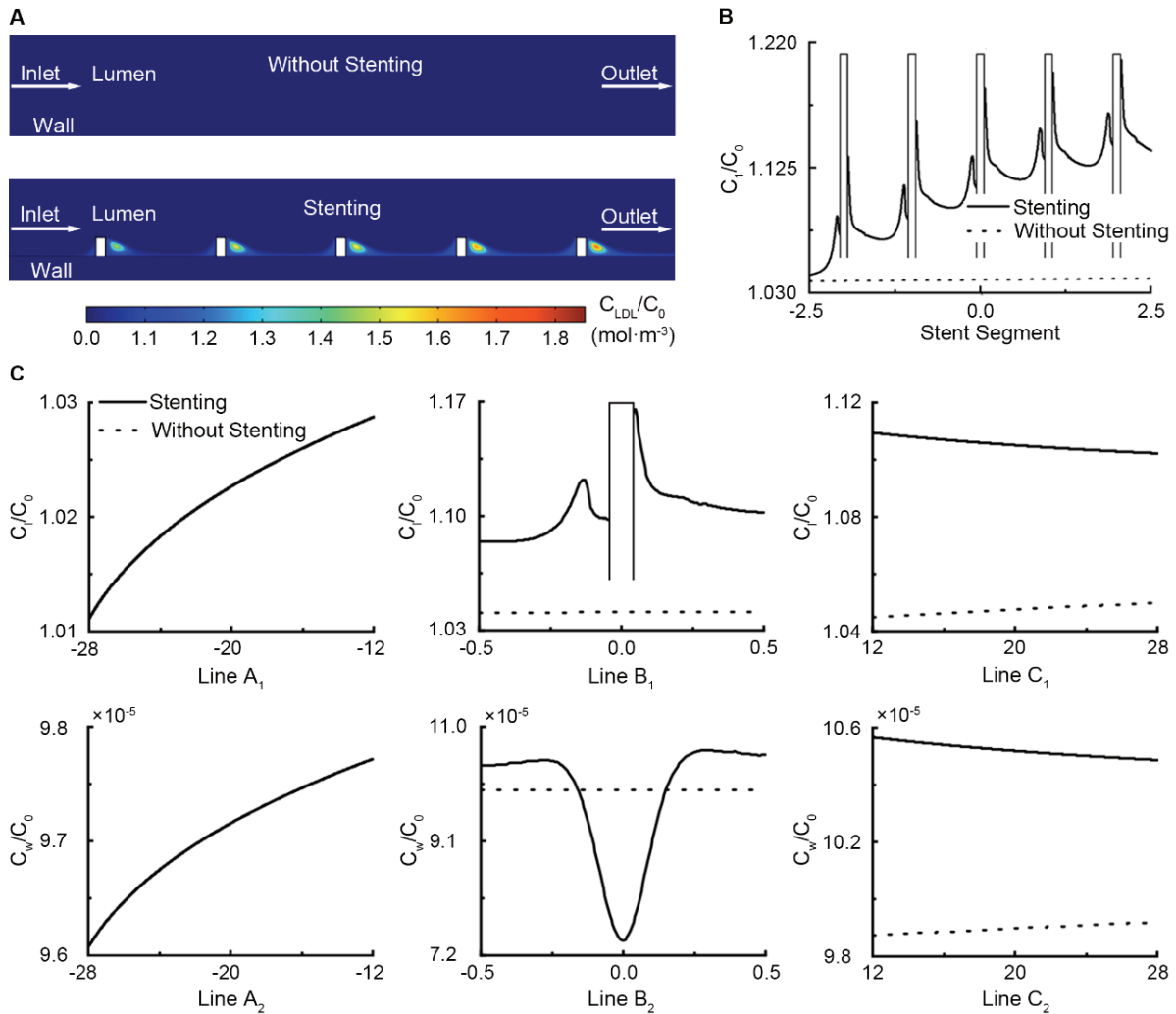


Fig. 2. Effect of stent implantation on the transport of LDL. A) Distribution of LDL in the coronary artery, B) The profile of LDL concentration on the luminal surface the model near the implanted stent. The solid black line is the artery after stenting, while the dashed line is the control case without stenting, C) The profile of LDL concentration at the representative lines

strut would further increase at the downstream struts, and the last strut is suffering from the highest LDL concentration. As shown in Fig. 2B, the protruded stent struts cause LDL concentration to rise sharply near the strut. The downstream stent struts would be obviously impacted by the downstream LDL concentration, and LDL concentration near struts would display a clear increase with the distance between the strut relative to the start one. LDL concentration would be relatively low in the start stent strut and be significantly elevated at the last one. The maximum value of LDL concentration near the end strut was 1.3 times higher than the start one.

To facilitate presenting the effect of stenting on the host artery, the representative lines on the luminal surface and in artery wall were selected and shown in Fig. 2C. It has been observed that the LDL concentration is almost the same both on the luminal

surface and within arterial wall, for the upstream region of the stented segment, while there is a large difference between models in the region of stented segment and downstream of that region. There is the largest fluctuation and high level of LDL concentration along the line B₁, which was by about 12% higher than the model without stenting. LDL concentration on the line B₂ slightly increased both at the upstream and downstream of the strut edge, while this curve shows a sharp decrease under the implanted strut in artery wall. Although LDL concentration tends to slowly decrease at downstream of stented segment, the significant difference between the cases with and without stent can still be observed, and this value in the case with stent is by at least 7% higher than the one without on luminal surface and in the arterial wall.

3.2. Effect of the conductivity hydraulic near the strut

In Figure 3A, the distribution of LDL for the host artery with different the hydraulic conductivities at the stented segment is shown. It is evident that compared to the healthy artery wall, the models with high hydraulic conductivity could gradually lead to high level of LDL concentration at the stented segment and downstream of that region. Nevertheless, these changes of LDL concentration due to high hydraulic conductivities is not noticeable in the most region of host arteries. The highest concentration for each model is located at the last strut downstream edge, which are the 1.67, 1.81 and 1.83, respectively. The curves shown in Fig. 3B further present the effect of the conductivity hydraulic on the distribution of LDL. As shown this figure, the upstream of stented segment shows no difference both on the luminal surface of arterial wall (Line A₁) and in the wall (Line A₂), while LDL concentration changes greatly at stented segment. Along Line B₁, the

maximum concentration is increased by approximate 6 and 10% for the models with 3- and 6-times hydraulic conductivity, respectively, compared to the healthy artery wall. And the maximum values are respectively increased by 6 and 10% along the Line B₂. Moreover, high hydraulic conductivity slightly increased the LDL concentration at the downstream of stented segment, but it slowly decreased with the distance relate to the starting stented segment.

3.3. Effect of the strut thickness

In Figure 4, the impact of strut thickness on the distribution of LDL in coronary is illustrated. As shown in Fig. 4A, the thick strut obviously increased the magnitude of LDL concentration at the stented segment and downstream of that region. The maximum LDL concentration in 122- μm strut case is approximately 22% for 146- μm strut and 30% for 162- μm strut. As evident from Fig. 4B, compared to the other cases, the change of LDL in 122- μm strut is more obviously near the

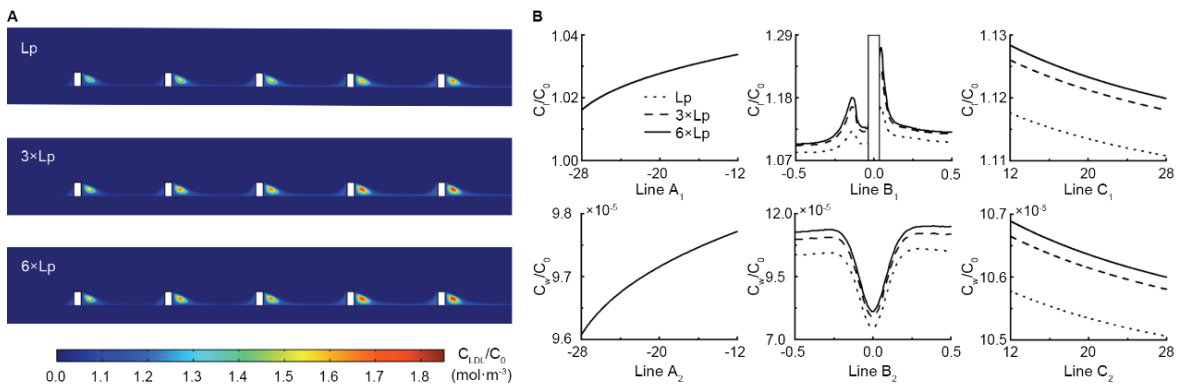


Fig. 3. Effect of the conductivity hydraulic on the transport of LDL: A) Distribution of LDL in the coronary artery, B) The profile of LDL concentration at the representative lines. L_p , $3 \times L_p$ and $6 \times L_p$ are one, three and six times larger than the conductivity hydraulic in the health artery

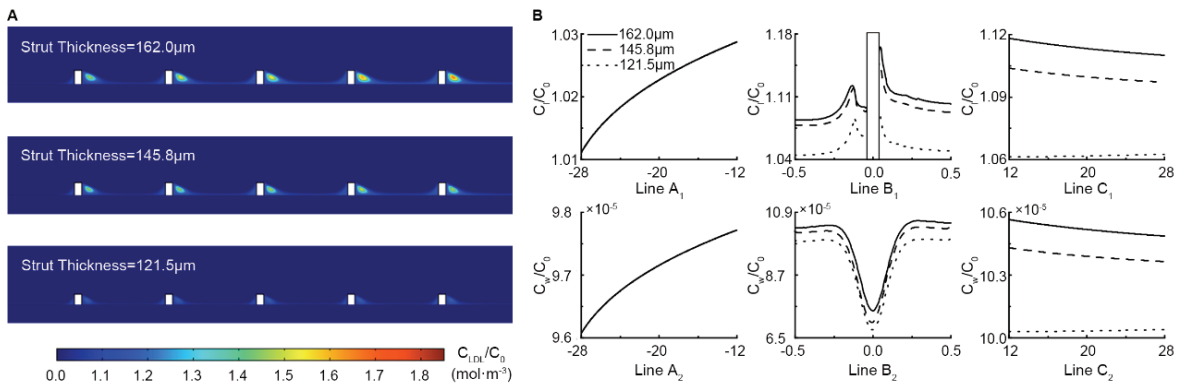


Fig. 4. Effect of strut thickness on the LDL distribution: A) Distribution of LDL in the coronary artery, B) The profile of LDL concentration along the representative lines

strut than others, and the maximum values decreased approximately by 6% for the thin strut on the line B₁ and by 10% on the line B₂. The maximum LDL concentration for 122- μm strut both on the line C₁ and line C₂ are by about 5% smaller than thicker cases.

3.4. Effect of strut spacing

In Figure 5A, the impact of strut spacing on the distribution of LDL in coronary artery is illustrated. The high LDL induced by strut protrusion clearly decreased with the large strut spacing, showing the lowest level at the last strut. Compared to small spacing (spacing = 1 mm), the maximum concentration of LDL for doubled spacing (spacing = 2 mm) was reduced from 1.67 to 1.60, and this value reduced to 1.55 when the strut spacing has quadrupled (spacing = 4 mm). The LDL concentration decreased by less than 5% both on the luminal surface and in artery wall when the strut spacing increased from 1 mm to 2 mm, while the maxi-

imum concentration reduced by more than 10% on the line B₁ for the quadrupled strut. Moreover, as evident from Fig. 5B, the average concentration in the stented segment dropped from 1.14 to 1.05 when the strut spacing increased from 1 mm to 4 mm.

3.5. Effect of the shape of strut

In Figure 6, the impact of streamline-strut on the LDL distribution in the coronary artery is illustrated. As evident from the figure, the streamline-strut greatly suppressed high LDL concentration both at the stented segment and the downstream, the maximum concentration near the last strut decreased by approximately 30% for the strut with streamline one, and the average concentration in the stented segment dropped to 1.05, as shown in Fig. 6. In addition, it can be clearly seen from Fig. 6B that the average concentration between each streamline stent struts is lower than that of non-streamline one.

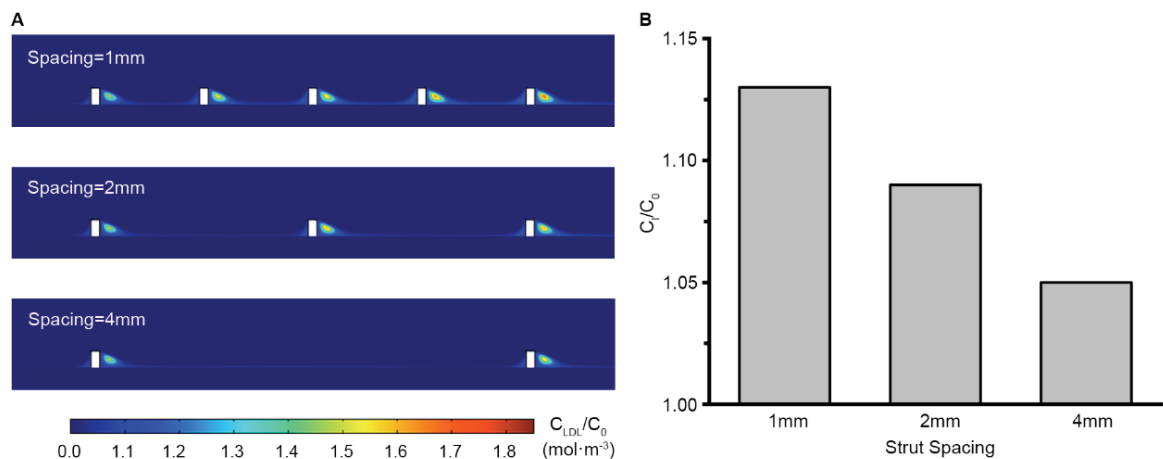


Fig. 5. Effect of strut spacing on the distribution of LDL: A) Distribution of LDL in the coronary artery, B) The profile of LDL concentration at the representative lines

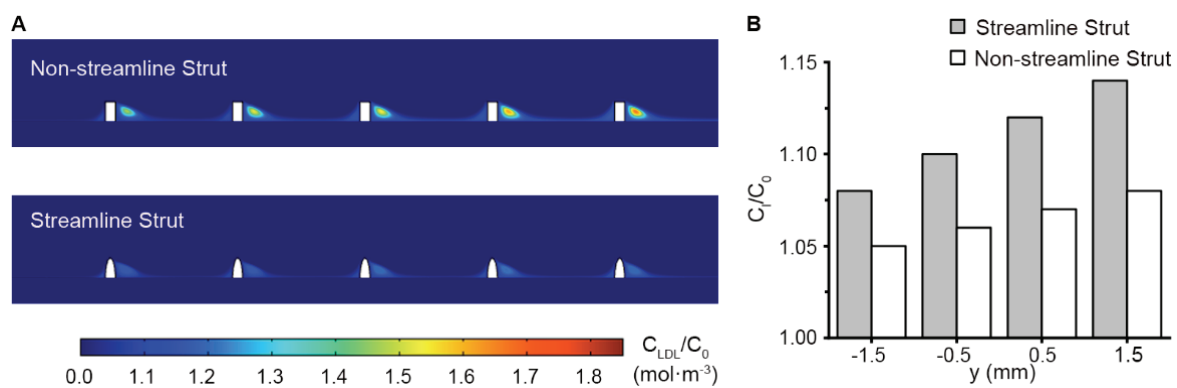


Fig. 6. Effect of strut shape on the distribution of LDL

4. Discussion

The clinical significance of percutaneous coronary interventions has been diminished due to the occurrence of late failures characterized by neoarteriosclerosis, stent restenosis and stent thrombosis. It is widely acknowledged that these events are closely linked to the adverse hemodynamics resulting from stent struts [23], [27]. Nevertheless, initial studies did not adequately elucidate the accelerated development of neoarteriosclerosis following stenting compared to atherosclerosis in native arteries, which is typically initiated and established by the excessive infiltration and accumulation of atherogenic lipoproteins in the arterial wall [4], [25]. The excessive infiltration and accumulation of atherogenic lipoproteins in the arterial wall are believed to be the initiators and drivers of atherosclerosis. This study proposes that the transport of low-density lipids after stenting may play a crucial role in the occurrence and progression of neoatherosclerosis.

The findings of this study demonstrate that the presence of a stent in the artery leads to elevated levels of LDL, particularly in the stented segment, with the distal edge of the last strut experiencing the highest concentration of LDL. This study demonstrated that the presence of a stent in the host artery resulted in elevated levels of LDL, particularly in the stented segment and the distal edge of the last strut. The excessive accumulation of LDL in these areas may contribute to the development of in-stent neoarteriosclerosis, a critical factor in the formation of lesions leading to late stent failure. This condition is characterized by an abundance of macrophages containing lipid droplets within the arterial wall. Atherosclerosis of the native coronary arteries is a common chronic condition that typically requires several decades to manifest clinically symptomatic symptoms. Conversely, neoarteriosclerosis tends to develop within months to years after the implantation of a stent, as supported by pathological and clinical imaging data [14]. The etiology of in-stent neoarteriosclerosis involves multiple factors.

The occurrence and development of in-stent events have been linked to the hemodynamic changes caused by stenting. Flow separation and stagnation flow around stent struts disrupt the local flow in the host artery, leading to vascular damage and adverse events [17], [23]. Previous research has identified a noteworthy inverse relationship between wall shear stress (WSS) and the concentration of low-density lipoprotein (LDL) on the luminal surface. Additionally, regions with low WSS may experience accelerated accumulation of LDL [18]. The present numerical study confirms that the LDL

concentration at the distal edge of the strut surpasses that at the proximal edge. We have observed a significant increase in LDL concentration downstream of the segment-treated stent, with the highest concentration found at the distal side of the stent. It is worth noting that there could be additional factors contributing to the occurrence of frequent clinical events following stenting, apart from elevated nonphysiological stress levels. Seo et al. [29] revealed that WSS exhibits a higher magnitude at the proximal region of the stent, while it decreases significantly towards the distal end. This finding confirms the accuracy and dependability of our numerical simulation.

Previous research has established a strong correlation between the distribution of LDL distribution and the hydraulic conductivity of the arterial walls, indicating their role in mass transport [3], [34]. The application of stenting introduces abnormal tension stress, squeezing pressure and flow shear stress, which can potentially inflict substantial harm to the arterial wall, thereby initiating adverse clinical symptoms. The augmentation of hydraulic conductivity and the partial impairment of the endothelial glycocalyx layer have been found to promote the infiltration and accumulation of atherogenic lipids, specifically LDL, within the arterial wall of the host. Experimental evidence has demonstrated that the compromised arterial wall exhibits heightened permeability and hydraulic conductivity, resulting in an increased buildup of macromolecules within the intima layer [12], [36]. Furthermore, the findings of the current study indicate that as hydraulic conductivity rises, there is a concurrent increase in the accumulation of LDL on the luminal surface and within the arterial wall. Furthermore, the arterial wall may experience significant damage, resulting in an elevation of LDL levels both on the surface of the lumen and within the vascular wall. It should be noted that although high LDL levels are not typically observed in the majority of the host artery due to its six times hydraulic conductivity, the accumulation of LDL caused by this increased conductivity can further expedite the development of in-stent events.

Additionally, the findings of this study indicate that the design of the stent is linked to the distribution and accumulation of LDL. The reduction in strut spacing and increase in strut size, along with the adoption of a non-streamline shape and longer stent length, would result in heightened adverse local hemodynamics within the host artery and significant damage to the arterial wall. Beier et al. [2] found that a smaller strut spacing would enlarge the area within the host arterial wall under low wall shear stress, and improved clinical outcomes have been reported following stenting with fewer struts

or wider strut spacing. Kolandaivelu and Kastrati demonstrated that thicker struts could exacerbate blood flow disturbances within the arterial lumen, increase the degree of separation, and expand the reflux area. The incidence of restenosis and late thrombosis was found to be higher in arteries treated with thick stents compared to those treated with thin stents [16], [26]. Poon et al. and Hisao et al. have suggested that the use of streamlined and thin stents can effectively mitigate flow disturbances, characterized by short distances of blood flow separation [28], [29]. The adverse hemodynamic conditions created by the stent design around the strut may alter the transport of LDL in the artery, resulting in elevated local LDL concentrations following stent placement. Furthermore, the occurrence of significant vascular endothelial damage caused by inadequate design or improper implantation leads to elevated hydraulic conductivity. This, in turn, facilitates the transportation of LDL from the lumen to the arterial wall, thereby amplifying the likelihood of adverse clinical events subsequent to stenting. The results underscore the critical importance of stent design. While ensuring sufficient structural support of vascular stents, it is essential to minimize the protrusion height within the lumen and increase the spacing between stent struts to achieve a more uniform and lower LDL concentration distribution. However, certain geometric configurations are sometimes unavoidable. For instance, large biodegradable stents, constrained by material properties, inherently require larger dimensions, which can increase the risks associated with implantation. In such cases, it becomes imperative to optimize both the implantation method and the overall stent structure to mitigate these risks effectively [6], [38].

Firstly, the numerical models were simplified to an idealized straight configuration, which does not account for the complex geometries observed in clinical scenarios. Furthermore, in addition to coronary arteries, other host vessels such as carotid and femoral arteries should also be investigated to derive more generalizable conclusions. Additionally, the potential impact of tissue prolapse between stent struts on LDL distribution was overlooked. Moreover, the hydraulic conductivity after different stent implantations was assumed as multiplied without measurement.

5. Conclusions

The process of intracoronary stenting has the potential to exert a synergistic effect on both the concentration and distribution of LDL in the host artery.

Factors such as increased severity of damage resulting from the intervention, narrower spacing between stents, thicker stent struts, and shorter stent length can exacerbate local infiltration and accumulation of LDL, thereby accelerating the development of neoarteriosclerosis, in-stent restenosis and late thrombosis.

Conflict of interest

The authors declare no competing interests.

Authors' contributions

Zhenmin Fan and Xiao Liu conceived the idea. Zhenmin Fan, Jialiang Yao and Kailei Liu conducted the analyses. Zhenmin Fan, Jialiang Yao, and Mingyuan Liu provided the data. Zhenmin Fan, Xia Ye and Xiaoyan Deng wrote the paper. All authors contributed to the writing and revisions.

Availability of data and materials

The datasets used and/or analyzed during the current study are available from the corresponding author on reasonable request.

Consent for publication

We consent for the publication of this work.

Acknowledgements

This work is supported by National Natural Science Research Foundation of China (No. 12372305, 12272153, 12202274, 11902126), Social Development Science and Technology Support Project of Changzhou (CE20235044), Changzhou Science and Technology Support Program (CJ20241077), Outstanding young backbone teacher of Jiangsu Qinglan Project, Zhongwu young innovative talents projection from Jiangsu Institute of Technology, and the Interdisciplinary Program of Shanghai Jiao Tong University (project number YG2022QN049).

References

- [1] BALOSSINO R., GERVASO F., MIGLIAVACCA F., DUBINI G., *Effects of different stent designs on local hemodynamics in stented arteries*, J. Biomech., 2008, 1053–1061.
- [2] BEIER S., ORMISTON J., WEBSTER M., CATER J., NORRIS S., MEDRANO-GRACIA P., *Hemodynamics in Idealized Stented Coronary Arteries: Important Stent Design Considerations*, Ann. Biomed. Eng., 2016, 315–329.
- [3] DENG X., MAROIS Y., HOW T., MERHI Y., KING M., GUIDOIN R., KARINO T., *Luminal surface concentration of lipoprotein (LDL) and its effect on the wall uptake of cholesterol by canine carotid arteries*, J. Vasc. Surg., 1995, 135–145.

- [4] FARB A., BURKE A.P., KOLOGDIE F.D., VIRMANI R., *Pathological mechanisms of fatal late coronary stent thrombosis in humans*, *Circulation*, 2003, 1701–1706.
- [5] FOIN N., LEE R.D., TORII R., GUITIERREZ-CHICO J.L., MATTESINI A., NIJER S., *Impact of stent strut design in metallic stents and biodegradable scaffolds*, *Int. J. Cardiol.*, 2014, 800–808.
- [6] GHARLEGGI R., WRIGHT H., LUVIO V., JEPSON N., LUO Z., SENTHURNATHAN A., *A multi-objective optimization of stent geometries*, *J. Biomech.*, 2021, 110575.
- [7] GRADUS-PIZLO I., BIGELOW B., MAHOMED Y., SAWADA S.G., RIEGER K., FEIGENBAUM H., *Left anterior descending coronary artery wall thickness measured by high-frequency transthoracic and epicardial echocardiography includes adventitia*, *Am. J. Cardiol.*, 2003, 27–32.
- [8] HYUN S., KLEINSTREUER C., ARCHIE J.P. Jr., *Computational particle-hemodynamics analysis and geometric reconstruction after carotid endarterectomy*, *Comput. Biol. Med.*, 2001, 365–384.
- [9] IQBAL J., GUNN J., SERRUYS P.W., *Coronary stents: historical development, current status and future directions*, *Br. Med. Bull.*, 2013, 193–211.
- [10] JAFFE R., STRAUSS B.H., *Late and very late thrombosis of drug-eluting stents: evolving concepts and perspectives*, *J. Am. Coll. Cardiol.*, 2007, 119–127.
- [11] JONER M., KOPPARA T., BYRNE R.A., CASTELLANOS M.I., LEWERICH J., NOVOTNY J., *Neoatherosclerosis in Patients with Coronary Stent Thrombosis: Findings from Optical Coherence Tomography Imaging (A Report of the PRESTIGE Consortium)*, *JACC Cardiovasc. Interv.*, 2018, 1340–1350.
- [12] KARNER G., PERKTOLD K., *Effect of endothelial injury and increased blood pressure on albumin accumulation in the arterial wall: a numerical study*, *J. Biomech.*, 2000, 709–715.
- [13] KIM H.J., VIGNON-CLEMENTEL I.E., COOGAN J.S., FIGUEROA C.A., JANSEN K.E., TAYLOR C.A., *Patient-specific modeling of blood flow and pressure in human coronary arteries*, *Ann. Biomed. Eng.*, 2010, 3195–3209.
- [14] KIMURA T., ABE K., SHIZUTA S., ODASHIRO K., YOSHIDA Y., SAKAI K., *Long-term clinical and angiographic follow-up after coronary stent placement in native coronary arteries*, *Circulation*, 2002, 2986–2991.
- [15] KIPSHIDZE N., DANGAS G., TSAPENKO M., MOSES J., LEON M.B., KUTRYK M., SERRUYS P., *Role of the endothelium in modulating neointimal formation: vasculoprotective approaches to attenuate restenosis after percutaneous coronary interventions*, *J. Am. Coll. Cardiol.*, 2004, 733–739.
- [16] KOLANDAIVELU K., SWAMINATHAN R., GIBSON W.J., KOLACHALAMA V.B., NGUYEN-EHRENREICH K.L., GIDDINGS V.L., *Stent thrombogenicity early in high-risk interventional settings is driven by stent design and deployment and protected by polymer-drug coatings*, *Circulation*, 2011, 1400–1409.
- [17] KOSKINAS K.C., CHATZIZISIS Y.S., ANTONIADIS A.P., GIANNOGLOU G.D., *Role of endothelial shear stress in stent restenosis and thrombosis: pathophysiologic mechanisms and implications for clinical translation*, *J. Am. Coll. Cardiol.*, 2012, 1337–1349.
- [18] KU D.N., GIDDENS D.P., ZARINS C.K., GLAGOV S., *Pulsatile flow and atherosclerosis in the human carotid bifurcation. Positive correlation between plaque location and low oscillating shear stress*, *Arteriosclerosis*, 1985, 293–302.
- [19] LI X., LIU X., ZHANG P., FENG C., SUN A., KANG H., *Numerical simulation of haemodynamics and low-density lipoprotein transport in the rabbit aorta and their correlation with atherosclerotic plaque thickness*, *J. R. Soc. Interface*, 2017.
- [20] LIU X., FAN Y., DENG X., *Effect of the endothelial glycocalyx layer on arterial LDL transport under normal and high pressure*, *J. Theor. Biol.*, 2011, 71–81.
- [21] LIU X., WANG L., WANG Z., LI Z., KANG H., FAN Y., *Bioinspired helical graft with taper to enhance helical flow*, *J. Biomech.*, 2016, 3643–3650.
- [22] NAKAZAWA G., VORPAHL M., FINN A.V., NARULA J., VIRMANI R., *One step forward and two steps back with drug-eluting-stents: from preventing restenosis to causing late thrombosis and nouveau atherosclerosis*, *JACC Cardiovasc Imaging*, 2009, 625–628.
- [23] NG J., BOURANTAS C.V., TORII R., ANG H.Y., TENEKECIOGLU E., SERRUYS P.W., FOIN N., *Local Hemodynamic Forces After Stenting: Implications on Restenosis and Thrombosis*, *Arterioscler. Thromb. Vasc. Biol.*, 2017, 2231–2242.
- [24] OTSUKA F., FINN A.V., YAZDANI S.K., NAKANO M., KOLOGDIE F.D., VIRMANI R., *The importance of the endothelium in atherothrombosis and coronary stenting*, *Nat. Rev. Cardiol.*, 2012, 439–453.
- [25] OTSUKA F., SAKAKURA K., YAHAGI K., JONER M., VIRMANI R., *Has our understanding of calcification in human coronary atherosclerosis progressed?*, *Arterioscler. Thromb. Vasc. Biol.*, 2014, 724–736.
- [26] PACHE J., KASTRATI A., MEHILLI J., SCHUHLEN H., DOTZER F., HAUSLEITER J., *Intracoronary stenting and angiographic results: strut thickness effect on restenosis outcome (ISAR-STEROE-2) trial*, *J. Am. Coll. Cardiol.*, 2003, 1283–1288.
- [27] PARK S.J., KANG S.J., VIRMANI R., NAKANO M., UEDA Y., *Intest neoatherosclerosis: a final common pathway of late stent failure*, *J. Am. Coll. Cardiol.*, 2012, 2051–2057.
- [28] POON E.K., BARLIS P., MOORE S., PAN W.H., LIU Y., YE Y., *Numerical investigations of the haemodynamic changes associated with stent malapposition in an idealised coronary artery*, *J. Biomech.*, 2014, 2843–2851.
- [29] SEO T., SCHACHTER L.G., BARAKAT A.I., *Computational study of fluid mechanical disturbance induced by endovascular stents*, *Ann. Biomed. Eng.*, 2005, 444–456.
- [30] STONE G.W., ELLIS S.G., COLOMBO A., DAWKINS K.D., GRUBE E., CUTLIP D.E., *Offsetting impact of thrombosis and restenosis on the occurrence of death and myocardial infarction after paclitaxel-eluting and bare metal stent implantation*, *Circulation*, 2007, 2842–2847.
- [31] SUN N., WOOD N.B., HUGHES A.D., THOM S.A., XU X.Y., *Fluid-wall modelling of mass transfer in an axisymmetric stenosis: effects of shear-dependent transport properties*, *Ann. Biomed. Eng.*, 2006, 1119–1128.
- [32] TADA Y., WADA K., SHIMADA K., MAKINO H., LIANG E.I., MURAKAMI S., *Roles of hypertension in the rupture of intracranial aneurysms*, *Stroke*, 2014, 579–586.
- [33] VINK H., DULING B.R., *Identification of distinct luminal domains for macromolecules, erythrocytes, and leukocytes within mammalian capillaries*, *Circ. Res.*, 1996, 581–589.
- [34] WADA S., KARINO T., *Theoretical prediction of low-density lipoproteins concentration at the luminal surface of an artery with a multiple bend*, *Ann. Biomed. Eng.*, 2002, 778–791.
- [35] WANG J., JIN X., HUANG Y., RAN X., LUO D., YANG D., *Endovascular stent-induced alterations in host artery mechanical environments and their roles in stent restenosis and late thrombosis*, *Regen. Biomater.*, 2018, 177–187.

- [36] WANG Z., LIU M., LIU X., SUN A., FAN Y., DENG X., *Hydraulic conductivity and low-density lipoprotein transport of the venous graft wall in an arterial bypass*, Biomed. Eng. Online, 2019, 50.
- [37] WANG Z., LIU X., KANG H., SUN A., FAN Y., DENG X., *Enhanced accumulation of LDLs within the venous graft wall induced by elevated filtration rate may account for its accelerated atherogenesis*, Atherosclerosis, 2014, 198–206.
- [38] XUE Y., LIU X., SUN A., ZHANG P., FAN Y., DENG X., *Hemodynamic Performance of a New Punched Stent Strut: A Numerical Study*, Artif. Organs, 2016, 669–677.
- [39] ZHANG D., XU P., QIAO H., LIU X., LUO L., HUANG W., *Carotid DSA based CFD simulation in assessing the patient with asymptomatic carotid stenosis: a preliminary study*, Biomed. Eng. Online, 2018, 31.